ChemComm

In situ SEIRAS analysis of enhanced photocatalytic carrier transfer to Pt cocatalyst induced by sacrificial reagents

Journal:	*ChemComm*
Manuscript ID	CC-COM-11-2024-005860.R4
Article Type:	Communication

ChemComm

COMMUNICATION

In situ SEIRAS analysis of enhanced photocatalytic carrier transfer to Pt cocatalyst induced by sacrificial reagents

Received 00th January 20xx,
Accepted 00th January 20xx

DOI: 10.1039/x0xx00000x

Shu Ashimura,[a] Ota Mori,[a] Reiya Konaka,[a] Takuya Iwai,[a] Chechia Hu,[b] Ke-Hsuan Wang,[c] Chien-Hsiang Chang,[d] Yuh-Lang Lee,[d] and Masaaki Yoshida*[,a,e]

In situ SEIRAS analyses revealed a peak shift of adsorbed CO on Pt cocatalysts supported on TiO_2 photocatalysts in the presence of sacrificial reagents. This observation suggests that charge separation from the photocatalysts to the cocatalysts was enhanced, leading to negative potential shifts that promote hydrogen evolution.

Ongoing population growth has led to the increased consumption of fossil fuels, which in turn has elevated greenhouse gas emissions. These emissions contribute to global warming, and so there is an urgent need to replace fossil fuels with clean energy sources. Photocatalytic water splitting[1] utilizing solar energy to produce hydrogen as an energy source has gained considerable attention in this regard. In this process, the catalyst absorbs sunlight to generate electrons and holes as excited charge carriers within the catalyst. These electrons and holes subsequently migrate to the surfaces of cocatalysts and participate in reactions that produce hydrogen and oxygen.

Research groups around the world are currently developing highly active photocatalysts for water splitting.[2] As an example, Domen et al. reported a maximum external quantum efficiency of 96% for overall water splitting under 350-360 nm light using Rh/Cr_2O_3[3] supported on Al-doped $SrTiO_3$.[4] In other work, Kudo and colleagues developed a La-doped $NiO/NaTaO_3$[5] photocatalyst that exhibited nine times higher photocatalytic activity than its undoped counterpart, achieving a maximum apparent quantum yield of 56% in response to 270 nm radiation.[6] This exploration of high-efficiency photocatalytic materials is ongoing and widespread,[7] although the functionality of such materials has not yet been fully evaluated.

In situ spectroscopy can allow the movement of excited carriers within a photocatalyst to be observed as a means of elucidating carrier dynamics.[8] Kamat and colleagues examined excited carriers within TiO_2 on Au nanoparticles in a thiol-crosslinked photocatalyst using UV-visible spectroscopy.[9] Other studies have employed X-ray,[10] UV[11] or visible-mid infrared[12] lasers in conjunction with time-resolved absorption spectroscopy to track the behaviour of excited carriers within photocatalytic materials. Ozawa et al. used time-resolved photoelectron spectroscopy to observe excited carriers on TiO_2 surfaces under vacuum.[13] Such studies demonstrate that many research groups have assessed excited carrier transfer in photocatalytic materials. However, there have been no reports of in situ observations of excited carrier transfer from photocatalysts to cocatalysts in solution. Furthermore, while sacrificial reagents are known to enhance photocatalytic activity through their structural properties, suppression of reverse hole transfer from the solution to the photocatalyst, and induced structural changes on the photocatalyst surface, their effects on the reaction sites of the cocatalyst remain unclear.[14]

When investigating photocatalyst activity, it is crucial to consider the reaction sites on cocatalysts, as it has been shown that the transfer of excited carriers to cocatalysts is closely associated with such sites.[15] Kondoh et al. observed the movement of holes from a $SrTiO_3$ photocatalyst to an oxygen evolution cocatalyst under steam using in situ conversion electron yield soft X-ray absorption spectroscopy.[16] We have also monitored the transfer of holes to oxygen evolution cocatalysts in various photocatalysts and photoelectrodes using in situ X-ray absorption spectroscopy.[17] In prior work, the functioning of reaction sites on a hydrogen evolution cocatalyst was examined by assessing the relationship between the vibrational frequency of CO molecules and the local electrode potential of the cocatalyst. This was accomplished using in situ attenuated total reflection surface-enhanced infrared absorption spectroscopy (ATR-SEIRAS) employing CO molecules as probes.[18] We have also previously used GaN single-crystal substrates as photoelectrode materials and observed the transfer of excited carriers from GaN photoelectrodes to Pt cocatalysts using in situ CO-probe SEIRAS.[19] Additionally, Kubota et al. monitored the transfer of excited electrons from various photocatalyst powders to Pt cocatalysts.[20] We also employed in situ CO-probe SEIRAS to evaluate the effect of the Pt/Si photoelectrode interface structure on the transfer of excited carriers to the Pt cocatalyst.[21] Such examinations

[a] Yamaguchi University, 2-16-1, Tokiwadai, Ube, Yamaguchi 755-8611, Japan
[b] National Taiwan University of Science and Technology, Daan Dist., Taipei City 106, Taiwan
[c] Sanyo-Onoda City University, 1-1-1, Sanyo-Onoda, Yamaguchi 756-0884 Japan
[d] National Cheng Kung University, No. 1, University Road, Tainan 70101, Taiwan
[e] Blue Energy Center for SGE Technology (BEST) of Yamaguchi University
† Electronic Supplementary Information (ESI) available.
See DOI: 10.1039/x0xx00000x

of excited carrier transfer can help to elucidate the functioning of cocatalysts, although more data are required.

The present study employed TiO_2, which exhibits high hydrogen evolution activity in response to UV light, as a model photocatalyst. In this work, the transfer of excited carriers from the TiO_2 photocatalyst to Pt acting as a hydrogen evolution cocatalyst was monitored in the presence of a sacrificial reagent using in situ CO-probe SEIRAS. Based on tracking changes in the local electrode potential of the Pt cocatalyst while varying the sacrificial reagent, the correlation between the activity of the Pt/TiO_2 photocatalyst and the reaction sites on the cocatalyst was determined.

Multiple characterization techniques were used to examine the surface morphology, elemental composition and chemical state of the Pt/TiO_2 photocatalyst (Pt:10wt%). Transmission electron microscopy images and particle size distribution of Pt nanoparticles (Fig. S1) along with X-ray diffraction data (Fig. S2) obtained at the Pt/TiO_2 interface confirm the presence of Pt nanoparticles on the TiO_2, which have diameters of several nanometers. The elemental composition of the Pt/TiO_2 was ascertained using energy dispersive X-ray spectroscopy (Fig. S3a) and wide-scan X-ray photoelectron spectroscopy (XPS) (Fig. S3b). The results confirmed that Pt particles had been photodeposited on the TiO_2. Narrow-scan Pt 4f XPS data (Fig. S4a) and Pt L_3-edge X-ray absorption fine structure (XAFS) analyses (Fig. S4b) were used to evaluate the chemical state of the Pt. These assessments suggested that the Pt on the TiO_2 was in a metallic state. Curve fitting of the Fourier transformed extended XAFS results (Fig. S5) established that the local structure of the Pt/TiO_2 included Pt-Pt and Pt-Ti shells. The effect of varying the sacrificial reagent on the activity of the photocatalyst was investigated by monitoring hydrogen generation in conjunction with exposure to UV-visible light (300-600 nm). These trials were performed in ultrapure water, an aqueous 15 vol% ethanol (EtOH) solution or an aqueous 15 vol% methanol (MeOH) solution (Fig. 1). A slight amount of hydrogen was generated when using ultrapure water, suggesting that the activity of the Pt/TiO_2 photocatalyst is quite low in this solution. In contrast, hydrogen evolution was observed with either the EtOH or MeOH solutions, with the two producing different quantities of this product. This difference in hydrogen output is attributed to the fact that MeOH is more easily oxidized electrochemically compared with EtOH, based on their redox potentials.[22] It appears that the MeOH solution more effectively promoted the hydrogen evolution reaction on the Pt cocatalyst.

ATR-SEIRAS analyses were carried out using a method similar to that employed in our previous study.[19, 21] In situ CO-probe SEIRAS data were acquired using a Fourier transform infrared spectrophotometer (FT/IR-4600, JASCO Co.) equipped with a mercury cadmium telluride detector. A reference spectrum was obtained with nitrogen saturation under dark conditions. Prior to each experiment, CO gas was bubbled through the solution for 15 min to allow CO molecules to adsorb on the Pt surfaces. The frequency changes of these adsorbed CO molecules were monitored utilizing an electrochemical cell connected to a Pt counter electrode and an Ag/AgCl (3 M NaCl) reference

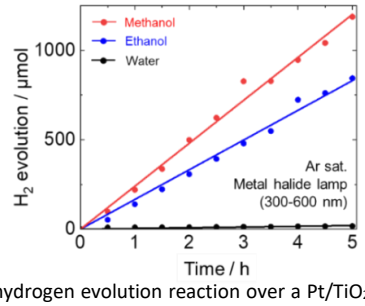

Fig. 1 The hydrogen evolution reaction over a Pt/TiO_2 photocatalyst in response to 300-600 nm light. The black, blue and red lines represent results obtained using ultrapure water, aqueous ethanol and aqueous methanol, respectively.

electrode. These trials were conducted in a 0.05 M aqueous H_2SO_4 solution saturated with CO while controlling the potential of the Pt electrode using a potentiostat (HA-151B; Hokuto Denko Co.) (Fig. S6a). In situ CO-probe SEIRAS assessments of the Pt/TiO_2 were performed in ultrapure water, an EtOH solution or a MeOH solution, both in the dark and with exposure to UV radiation (less than 10^2 mW/cm^2) (ULEDN-101, NS Lighting Co.) at steady state (Fig. S7).

In preliminary work, the relationship between the stretching frequency of CO molecules adsorbed on a Pt electrode and the electrode potential of the Pt was investigated in the absence of light. Variations in the SEIRA spectra with changes in the potential under dark conditions are presented in Fig. S6b. At a Pt electrode potential of -0.24 V vs. RHE, the CO peak was located at 2035 cm^{-1}. However, as the potential was increased, this peak shifted to higher frequencies and a position of 2065 cm^{-1} was observed at 0.76 V vs. RHE. Plotting the peak position as a function of the potential (Fig. S6c) indicated a linear correlation with a slope of 28 cm^{-1} V^{-1}. This value is in good agreement with the slopes obtained in prior studies[18a] and demonstrates that a 1.0 V increase in the electrode potential shifted the CO peak by 28 cm^{-1} to higher frequency. These frequency changes were associated with back-donation of electrons from the Pt electrode to the $2\pi^*$ antibonding orbital of the CO molecules and were also affected by the surrounding electric field. Therefore, based on this relationship, changes in the local electrode potential at the Pt cocatalyst on the TiO_2 photocatalyst could be roughly estimated. Please note that H_2SO_4 solution was adopted for this tentative estimation of electrode potential of Pt cocatalysts, instead of a neutral aqueous solution due to the problem of electrochemical measurements (Fig. S8). Furthermore, the bare Pt electrode was conducted for the estimation, not using Pt/TiO_2 powder as the electrode because of the low conductivity (Fig. S9).

Fig. 2 presents spectra reflecting the transfer of excited carriers from the TiO_2 photocatalyst to the Pt cocatalyst under UV light in ultrapure water, an EtOH solution or a MeOH solution. In ultrapure water, the CO peak appeared at 2065 cm^{-1} under dark conditions but shifted approximately 3 cm^{-1} to the lower frequency side upon irradiation. When the irradiation was stopped, the CO peak returned to its original position (Fig. 2a). These results suggest that a small number of excited electrons accumulated in the Pt cocatalyst. The local electrode potential change of the Pt cocatalyst at this time was tentatively

evaluated as 0.11 V by the slope of the proportional relationship in Fig. S6c. In the presence of EtOH as a sacrificial reagent, the frequency of the CO molecules on the Pt cocatalyst was shifted by approximately 7 cm^{-1} to lower frequency upon irradiation (Fig. 2b). From this outcome, it is evident that the photogenerated holes were consumed in oxidation reactions with the aqueous EtOH solution on the TiO_2 photocatalyst. This phenomenon promoted charge separation and facilitated the transfer of excited electrons to the Pt cocatalyst, thereby shifting its local potential towards more negative values. Based on the slope derived from the proportional relationship in Fig. S6c and the variations in the potential of the Pt cocatalyst, it appears that the electrode potential of the Pt cocatalyst in the EtOH solution was shifted negatively by approximately 0.25 V. In the case of the trials in the MeOH solution, a shift of approximately 11 cm^{-1} to lower frequency was observed during irradiation (Fig. 2c), indicating a larger change than that in the EtOH solution. This result shows the property of MeOH being more easily oxidized electrochemically allowed more holes to be captured, suppressing the recombination reaction with excited electrons. Consequently, the excited electrons moved to the Pt cocatalyst, causing a significant change in the local electrode potential. The potential change of the Pt cocatalyst in the MeOH solution was roughly estimated to be on the order of 0.39 V, representing the largest change observed during the in situ CO-probe SEIRAS analyses in the presence of sacrificial reagents. Thus, the in situ CO-probe SEIRAS results established that the trapping of holes by the oxidation reaction of the sacrificial reagent affected the transfer of excited carriers within the photocatalyst and increased the change in the local electrode potential of the Pt cocatalysts. It should be noted that sacrificial reagents such as methanol and ethanol did not affect the SEIRA spectra of CO adsorption on the Pt cocatalyst, because CO gas was initially adsorbed onto Pt cocatalyst using a CO-saturated aqueous solution (Fig. S10). On the other hand, note that there is the possibility that CO may block the hydrogen generation sites on the Pt cocatalyst during SEIRAS measurements, because the CO adsorption prevent electrochemical hydrogen evolution on the Pt electrode (Fig. S11). In addition, the magnitude of the shift of the CO peak in SEIRAS measurements varies with light intensity, suggesting that the local electrode potential at the Pt cocatalyst is affected by the number of photons absorbed by the photocatalyst (Figure S12). Further investigation is needed to clarify the relationship between electron accumulation and hydrogen formation rate through future systematic studies involving variations in light intensity.

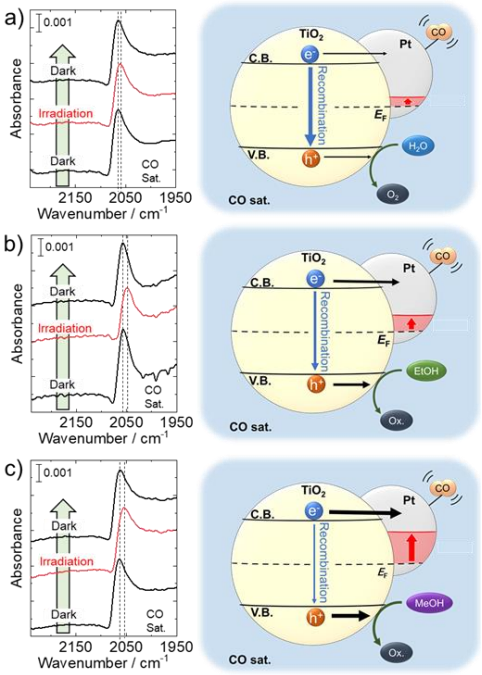

Fig. 2 In situ SEIRA spectra of CO molecules adsorbed on Pt cocatalyst on TiO_2 photocatalyst in a) ultrapure water, b) aqueous EtOH solution and c) aqueous MeOH solution. These spectra were obtained at steady state, under CO-saturated conditions, both in the dark and with irradiation. The diagram shows the elementary processes occurring during excited carrier transfer within the Pt/TiO_2 photocatalyst in response to light and indicates the valence band (V.B.), conduction band (C.B.) and Fermi level (E_F).

Based on these in situ CO-probe SEIRAS results, a mechanism for the hydrogen evolution reaction facilitated by this Pt/TiO_2 photocatalyst in the presence of a sacrificial reagent can be proposed. In this process, holes are consumed in oxidation reactions with the sacrificial reagent on the surface of the TiO_2 photocatalyst, facilitating the transfer of charge-separated excited electrons to the Pt cocatalyst. Hence, the local electrode potential is shifted negatively due to the increased density of excited electrons within the Pt cocatalyst. This negative shift probably reaches the potential required for the hydrogen evolution potential (0 V vs. RHE), promotes the hydrogen evolution reaction on the Pt cocatalysts. It is therefore apparent that enhancing the transfer of excited carriers to the cocatalyst by using a sacrificial reagent is a crucial aspect of improving photocatalytic activity. The technique used herein also allowed the shift in the local electrode potential of the cocatalyst to be estimated. This represents a useful means of assessing the transfer of excited carriers and could thereby aid in the development of highly active water-splitting photocatalysts.

In conclusion, in situ CO-probe SEIRAS analyses using CO molecules as probes were employed to observe the transfer of excited electrons from a TiO_2 photocatalyst to a Pt cocatalyst. The results suggest that photogenerated holes within the TiO_2 photocatalyst were consumed in oxidation reactions with the sacrificial reagent on the surface of the material. This process promoted the transfer of excited electrons to the Pt cocatalyst such that the local electrode potential was negatively shifted. As more holes were captured by the oxidation reaction of the sacrificial reagent, further enhancing the transfer of excited electrons to the Pt cocatalyst and increasing the negative shift in the local electrode potential. This negative shift that ultimately resulted from the sacrificial reagent significantly increased the hydrogen evolution reaction rate on the cocatalyst.

XAFS analyses were conducted at the KEK-PF (2022G609) and the SPring-8 (2024B1694, 2023B1636). This study was supported by JSPS KAKENHI (B) (21H02050) and JST SPRING (JPMJSP2111) and the YU Fund. The authors thank Prof. Yamakata (Okayama Univ.), A. N., Y. Y., T. Tonosaki, and Prof. Sakata (Yamaguchi Univ.) for their support.

Conflicts of interest

There are no conflicts to declare.

Data availability

The data that support the findings of this study are available from the corresponding author, [M. Y.], upon reasonable request.

Notes and references

1. a)S. Chen, T. Takata and K. Domen, *Nat Rev Mater*, 2017, **2**, 17050; b)A. Kudo and Y. Miseki, *Chem. Soc. Rev.*, 2009, **38**, 253-278; c)K. Sayama, A. Nomura, T. Arai, T. Sugita, R. Abe, M. Yanagida, T. Oi, Y. Iwasaki, Y. Abe and H. Sugihara, *J. Phys. Chem. B*, 2006, **110**, 11352-11360; d)R. Abe, M. Higashi, K. Sayama, Y. Abe and H. Sugihara, *J. Phys. Chem. B*, 2006, **110**, 2219-2226; e)Y. Goto, T. Hisatomi, Q. Wang, T. Higashi, K. Ishikiriyama, T. Maeda, Y. Sakata, S. Okunaka, H. Tokudome, M. Katayama, S. Akiyama, H. Nishiyama, Y. Inoue, T. Takewaki, T. Setoyama, T. Minegishi, T. Takata, T. Yamada and K. Domen, *Joule*, 2018, **2**, 509-520; f)L. Lin, Y. Ma, J. J. M. Vequizo, M. Nakabayashi, C. Gu, X. Tao, H. Yoshida, Y. Pihosh, Y. Nishina, A. Yamakata, N. Shibata, T. Hisatomi, T. Takata and K. Domen, *Nat Commun*, 2024, **15**, 397; g)A. Ishikawa, T. Takata, J. N. Kondo, M. Hara, H. Kobayashi and K. Domen, *J. Am. Chem. Soc.*, 2002, **124**, 13547-13553.
2. a)Z. Wang, Y. Inoue, T. Hisatomi, R. Ishikawa, Q. Wang, T. Takata, S. Chen, N. Shibata, Y. Ikuhara and K. Domen, *Nat Catal*, 2018, **1**, 756-763; b)X. Wang, K. Maeda, X. Chen, K. Takanabe, K. Domen, Y. Hou, X. Fu and M. Antonietti, *J. Am. Chem. Soc.*, 2009, **131**, 1680-1681; c)R. Abe, *J. Photochem. Photobiol. C: Photochem. Rev.*, 2010, **11**, 179-209; d)Q. Wang, T. Hisatomi, Q. Jia, H. Tokudome, M. Zhong, C. Wang, Z. Pan, T. Takata, M. Nakabayashi, N. Shibata, Y. Li, I. D. Sharp, A. Kudo, T. Yamada and K. Domen, *Nature Mater*, 2016, **15**, 611-615; e)L. Rengui, Z. Fuxiang, W. Donge, Y. Jingxiu, L. Mingrun, Z. Jian, Z. Xin, H. Hongxian and L. Can, *Nat. Commun.*, 2013, **4**, 1432-1432; f)Y. Li, L. Zhang, A. Torres-Pardo, J. M. González-Calbet, Y. Ma, P. Oleynikov, O. Terasaki, S. Asahina, M. Shima, D. Cha, L. Zhao, K. Takanabe, J. Kubota and K. Domen, *Nat Commun*, 2013, **4**.
3. a)K. Maeda, K. Teramura, D. Lu, N. Saito, Y. Inoue and K. Domen, *J. Phys. Chem. C*, 2007, **111**, 7554-7560; b)A. Xiong, T. Yoshinaga, T. Ikeda, M. Takashima, T. Hisatomi, K. Maeda, T. Setoyama, T. Teranishi and K. Domen, *Eur. J. Inorg. Chem.*, 2013, **2014**, 767-772.
4. a)H. Nishiyama, T. Yamada, M. Nakabayashi, Y. Maehara, M. Yamaguchi, Y. Kuromiya, Y. Nagatsuma, H. Tokudome, S. Akiyama, T. Watanabe, R. Narushima, S. Okunaka, N. Shibata, T. Takata, T. Hisatomi and K. Domen, *Nature*, 2021, **598**, 304-307; b)T. Takata, J. Jiang, Y. Sakata, M. Nakabayashi, N. Shibata, V. Nandal, K. Seki, T. Hisatomi and K. Domen, *Nature*, 2020, **581**, 411-414.
5. a)H. Kato and A. Kudo, *J. Phys. Chem. B*, 2001, **105**, 4285-4292; b)Q. Zhang, Z. Li, S. Wang, R. Li, X. Zhang, Z. Liang, H. Han, S. Liao and C. Li, *ACS Catal.*, 2016, **6**, 2182-2191.
6. H. Kato, K. Asakura and A. Kudo, *J. Am. Chem. Soc.*, 2003, **125**, 3082-3089.
7. a)K. Maeda and K. Domen, *J. Phys. Chem. Lett.*, 2010, **1**, 2655-2661; b)M. Higashi, R. Abe, K. Teramura, T. Takata, B. Ohtani and K. Domen, *Chem. Phys. Lett.*, 2008, **452**, 120-123; c)R. M. Navarro Yerga, M. C. Álvarez Galván, F. del Valle, J. A. Villoria de la Mano and J. L. G. Fierro, *ChemSusChem*, 2009, **2**, 471-485; d)Q. Wang, M. Nakabayashi, T. Hisatomi, S. Sun, S. Akiyama, Z. Wang, Z. Pan, X. Xiao, T. Watanabe, T. Yamada, N. Shibata, T. Takata and K. Domen, *Nature Mater*, 2019, **18**, 827-832; e)M. G. Kibria, F. A. Chowdhury, S. Zhao, B. AlOtaibi, M. L. Trudeau, H. Guo and Z. Mi, *Nat Commun*, 2015, **6**.
8. a)T. Tachikawa, S. Yamashita and T. Majima, *J. Am. Chem. Soc.*, 2011, **133**, 7197-7204; b)A. J. Cowan, C. J. Barnett, S. R. Pendlebury, M. Barroso, K. Sivula, M. Gratzel, J. R. Durrant and D. R. Klug, *J. Am. Chem. Soc.*, 2011, **133**, 10134-10140.
9. V. Subramanian, E. E. Wolf and P. V. Kamat, *J. Am. Chem. Soc.*, 2004, **126**, 4943-4950.
10. Y. Uemura, D. Kido, Y. Wakisaka, H. Uehara, T. Ohba, Y. Niwa, S. Nozawa, T. Sato, K. Ichiyanagi, R. Fukaya, S. Adachi, T. Katayama, T. Togashi, S. Owada, K. Ogawa, M. Yabashi, K. Hatada, S. Takakusagi, T. Yokoyama, B. Ohtani and K. Asakura, *Angew Chem Int Ed Engl*, 2016, **55**, 1364-1367.
11. B. Moss, Q. Wang, K. T. Butler, R. Grau-Crespo, S. Selim, A. Regoutz, T. Hisatomi, R. Godin, D. J. Payne, A. Kafizas, K. Domen, L. Steier and J. R. Durrant, *Nat. Mater.*, 2021, **20**, 511-517.
12. A. Yamakata, M. Kawaguchi, N. Nishimura, T. Minegishi, J. Kubota and K. Domen, *J. Phys. Chem. C*, 2014, **118**, 23897-23906.
13. K. Ozawa, M. Emori, S. Yamamoto, R. Yukawa, S. Yamamoto, R. Hobara, K. Fujikawa, H. Sakama and I. Matsuda, *J Phys Chem Lett*, 2014, **5**, 1953-1957.
14. a)C. Fu, F. Li, J. Zhang, D. Li, K. Qian, Y. Liu, J. Tang, F. Fan, Q. Zhang, X. Q. Gong and W. Huang, *Angew Chem Int Ed Engl*, 2021, **60**, 6160-6169; b)M. Yasuda, T. Matsumoto and T. Yamashita, *Renewable and Sustainable Energy Reviews*, 2018, **81**, 1627-1635; c)Z. Chen, Q. Zhang and Y. Luo, *Angew Chem Int Ed Engl*, 2018, **57**, 5320-5324; d)K. Sathiyan, R. Bar-Ziv, V. Marks, D. Meyerstein and T. Zidki, *Chemistry*, 2021, **27**, 15936-15943.
15. J. Yang, D. Wang, H. Han and C. Li, *Acc. Chem. Res.*, 2013, **46**, 1900-1909.
16. Z. Wang, R. Toyoshima, M. Yoshida, K. Mase and H. Kondoh, *J. Phys. Chem. C*, 2024, **128**, 9193-9201.
17. a)M. Yoshida, T. Yomogida, T. Mineo, K. Nitta, K. Kato, T. Masuda, H. Nitani, H. Abe, S. Takakusagi, T. Uruga, K. Asakura, K. Uosaki and H. Kondoh, *J. Phys. Chem. C*, 2014, **118**, 24302-24309; b)M. Yoshida, N. Gon, S. Maeda, T. Mineo, K. Nitta, K. Kato, H. Nitani, H. Abe, T. Uruga and H. Kondoh, *Chem. Lett.*, 2014, **43**, 1725-1727; c)M. Yoshida, T. Yomogida, T. Mineo, K. Nitta, K. Kato, T. Masuda, H. Nitani, H. Abe, S. Takakusagi, T. Uruga, K. Asakura, K. Uosaki and H. Kondoh, *Chem. Commun.*, 2013, **49**, 7848-7850.
18. a)G. Samjeské, K.-i. Komatsu and M. Osawa, *J. Phys. Chem. C*, 2009, **113**, 10222-10228; b)A. Yamakata, T. Uchida, J. Kubota and M. Osawa, *J. Phys. Chem. B*, 2006, **110**, 6423-6427.
19. M. Yoshida, A. Yamakata, K. Takanabe, J. Kubota, M. Osawa and K. Domen, *J. Am. Chem. Soc.*, 2009, **131**, 13218-13219.
20. X. Lu, A. Bandara, M. Katayama, A. Yamakata, J. Kubota and K. Domen, *J. Phys. Chem. C*, 2011, **115**, 23902-23907.
21. S. Ashimura, R. Konaka, T. Suginaga, K. Harada, A. Yamakata, C. Hu, H. N. Catherine, K.-H. Wang, T. Kawai and M. Yoshida, *J. Taiwan Inst. Chem. Eng.*, 2024, **158**.
22. L. T. Thanh, K. Okitsu, L. V. Boi and Y. Maeda, *Catalysts*, 2012, **2**, 191-222.

The data that support the findings of this study are available from the corresponding author, [M. Y.], upon reasonable request.